Image-based 3D Mapping of Rebar Location for Automated Assessment of Safe Drilling Areas Prior to Placing Embedments in Concrete Bridge Decks

Mani Golparvar-Fard[1],Behshad Ghadimi[2], Kamel S. Saidi[3], Geraldine S. Cheok[3], Marek Franaszek[3], and Robert R. Lipman[3]

[1] Assistant Professor, Vecellio Construction Eng. and Mgmt., Via Dept. of Civil and Env. Eng., and Myers-Lawson School of Construction, Virginia Tech, Blacksburg, VA; PH (540) 231-7255; FAX (540) 231-7532; email: golparvar@vt.edu

[2] PhD Student, Vecellio Construction Eng. and Mgmt., Via Dept. of Civil and Env. Eng., and Myers-Lawson School of Construction, Virginia Tech, Blacksburg, VA; PH (714) 400-1122; FAX (540) 231-7532; email: bag@vt.edu

[3] National Institute of Standards and Technology, Gaithersburg, MD; PH (301) 975-6069; FAX (301) 869-6275; emails: {kamel.saidi, cheok, marek.franaszek, robert.lipman}@nist.gov

ABSTRACT

This paper presents a new image-based approach for 3D mapping the locations of the rebar and embedded components in a railway bridge deck prior to placement of concrete. Our approach enables practitioners to quickly and automatically identify where the rebar and other underlying components are within the bridge decks, locate safe and unsafe drilling area, and create a valuable documentation for future retrofit or rehabilitation of the concrete bridge decks. In the proposed method, digital images collected along the rebar cage prior to placement of concrete are processed to automatically generate a 3D point cloud. Using a set of control points, the reconstructed point cloud is transformed into the site coordinate system. Next, a pattern recognition algorithm identifies the rebar locations. A cell-based map of the underlying structure is generated and the occupancies of the cells are automatically detected and visualized using color. Impact of the number of images and control points on the accuracy and density of the image-based 3D reconstruction, registration, and automated recognition of the rebar locations and safe/unsafe cells are studied in detail. Results of our experiments show the promise of applying this low-cost approach in practice.

INTRODUCTION

Placing embeds into a reinforced concrete structure after concrete is poured without damaging the reinforcement bars (rebar) is an industry wide challenge. In concrete structures such as bridge decks and post-tensioned concrete floors, damaging rebar may compromise structural integrity, may initiate a point for reinforcement corrosion, and result in considerable rework. Although negative impressions for the embeds can be made by placing various objects such as wooden dowels or steel rods into the rebar cage prior to pouring the concrete (and removing them once the concrete has partially or fully set), this practice is labor intensive, time consuming, and may jeopardize worker safety. Not only does inserting wooden dowels or other negatives into the rebar increase the congestion during placement of concrete by creating honeycombs and voids, but they may also move due to work crews walking on them and to the hydrostatic pressure of the concrete. Moreover, removing the

negatives is challenging and time-consuming due to dowels being covered by concrete; furthermore, for removal, two drill bits are required. One drill bit is used to remove the wooden dowel from the concrete, and then a masonry drill bit with slightly larger diameter is used to drill out the residuals of the wooden dowel. Figure 1 shows the current challenges associated with placement of embeds in concrete bridge decks.

The alternative method is to systematically and digitally map the locations of the rebar layers including the rebar-free spaces prior to concrete pouring. This can help measure and mark the locations for the embedments after the concrete is placed. This method eliminates the time and cost required to place the wooden dowels within the steel reinforcement mats and to remove them from the cured concrete. Moreover, by removing the obstacles concrete can freely flow within the rebar cage. In addition, digital maps of the reinforcement locations would be a valuable tool for future retrofit or repair of the railway decks.

Figure 1: Current time-consuming and labor-intensive practice of placing wooden dowels

Potential technologies that can efficiently and accurately create a 3D map of rebar and embedded objects prior to placement of concrete and help identify their locations include laser scanning, conventional photogrammetry techniques along with more recent image-based 3D reconstruction approaches. Among these alternatives, image-based 3D reconstruction methods such as Golparvar-Fard et al. (2011) can be very beneficial as it only needs a low-cost digital consumer camera, does not need calibration (which is typically a requirement in conventional photogrammetry) and expertise for operation, and can be easily applied to wider areas.

In this paper, we present a method based on an image-based 3D reconstruction algorithm. In our approach, a dense 3D point cloud model of the rebar and embedded objects are initially created. The point cloud is transformed to the site coordinate system using a control-based registration process. The outcome is placed into a new algorithm that can detect rebar and identify safe and unsafe drilling cells (openings between rebar). Finally, the safe and unsafe drilling areas can be modeled using an IFC (Industry Foundation Classes)-based Building Information Model (BIM) representation which is jointly visualized along with the point cloud and collected imagery in an augmented reality environment similar to Golparvar-Fard et al. (2009).

In the following sections, we first overview the current 3D mapping techniques, and discuss the objectives and the scope of the project. Next, the research method and the systematic validation process to verify the applicability of our approach is presented. Finally the contributions and practical benefits of this work are discussed.

BACKGROUND ON PRE-CONCRETE MAPPING TECHNIQUES

Laser Scanning

The use of laser scanning to locate rebar prior to pouring concrete does not appear to be common practice or it has not been widely documented. Little published research (Whitfield 2010) was identified during the literature review. However, the use of laser scanning in construction for other applications has been documented extensively in various studies (Tang et al. 2010, Cheok 2006). The laser scanners can produce high density point clouds that can be extremely useful for 3D mapping. However, the main limitations of laser scanners include the time to acquire the data and their size which limits their mobility (although newer laser scanners are more compact, it is still problematic to locate the scanner within the rebar cage to capture the lower rebar layers) and hence may not generate a dense point cloud of the lower rebar layers which is critical in our study. Other limitations of the 3D imaging laser scanning method are mixed pixel phenomenon, range errors for thin structures, range jumps at reflectance and color boundaries, and large errors due to specular reflection (Golparvar-Fard et al. 2011b, and Tang et al. 2010).

Image-based 3D Reconstruction and Conventional Photogrammetry

Image-based 3D reconstruction or photogrammetry has been applied to various construction scenarios and recently at a more accelerated pace due to advances in digital photography, the low cost of memory, and the increasing network bandwidths. Conventional photogrammetric techniques use high-resolution analog cameras and provide accurate models comparable to those of laser scanning systems, but their spatial point density is more limited and may initially require application of markers for calibration (Golparvar-Fard et al. 2011a). These conventional techniques can be restricted in camera rotations, range of the focal length, and analysis of the orientation data.

Due to recent developments in automated feature detection and matching techniques such as Scale Invariant Feature Transforms (SIFT) (Lowe 2004) and based on structure from motion (SfM) techniques, several research groups have developed systems which aim to automatically recover camera calibration information and reconstruct a sparse 3D representation of the scene geometry. An example of such techniques is the Phototour algorithm of Snavely et al. (2006), which is the backbone of the Microsoft Photosynth[1] system. The SfM techniques not only reconstruct a sparse representation of the scene, but also calibrate cameras up to an unknown scaling factor. Using calibration information derived from the SfM algorithm, several techniques such as Golparvar-Fard et al. (2011) and Furukawa and Ponce (2010) have proposed a new image-based 3D modeling pipeline which takes a collection of unordered and uncalibrated images and generates dense point clouds. Given the availability of unordered photo collections on construction sites, and the need for fully automated systems, such 3D reconstruction techniques have the potential to be

[1] Certain trade names and company products are mentioned in the text or identified in an illustration in order to adequately specify the experimental procedure and equipment used. In no case does such an identification imply recommendation or endorsement by NIST, nor does it imply that the products are necessarily the best available for the purpose.

the most useful approach for 3D construction applications. Hence, in this study, the proposed pipeline is used as part of the overall process to generate the necessary initial point cloud.

RESEARCH OBJECTIVES

This research explores application of unstructured collections of digital images to automatically map rebar and embedments in 3D and visualize rebar location and occupied/empty spaces for post-concrete identification of safe vs. unsafe drilling locations. Given a collection of uncalibrated and unstructured imagery, our goal is to automatically reconstruct a 3D point cloud model and transform it to the site coordinate system using a control-based registration process. A new method is created to detect rebar location and identify safe/unsafe drilling areas. The safe/unsafe drilling areas are visualized using an IFC-based BIM along with the point cloud model in an augmented reality environment. The results of this visualization process can be projected on the concrete surface by laser projector. In this paper, the impact of the number of images and control points per unit of area on the accuracy and completeness of the point cloud, and the accuracy of registration and identification of safe/unsafe drilling areas are tested and demonstrated in the National Institute of Standards and Technology (NIST) Intelligent and Automated Construction Job Site Testbed (IACJS) (Saidi et al. 2011).

IMAGE-BASED 3D MAPPING AND SAFE DRILLING IDENTIFICATION

In our work, we assume a collection of uncalibrated and unstructured images are available. Using a streamlined image-based 3D reconstruction (Golparvar-Fard et al. 2011a) which consists of Structure-from-Motion (SfM), Multi-View Stereo (MVS), and Voxel Coloring/Labeling (VCL), a dense 3D point cloud of the rebar and embedments are initially created. Next, using a control-based registration process the dense point cloud is transformed into the Euclidean site coordinate system. Figure 2 shows the registration targets that can be used in practice. In this case, the site coordinates of these targets are predefined using surveying techniques.

Since the scale of the point cloud reconstructed using uncalibrated imagery is unknown, this transformation includes Rotation (R), Translational offset (T), and a uniform Scale (s) (i.e.,seven degree-of-freedom (DOF)). Three points known in both coordinate systems are theoretically sufficient to determine these seven unknowns. However, in practice, these measurements are not always exact and using more than three points can reduce the registration error. Let n be the number of rebar targets that will be used for registration of the point cloud into the site coordinate system. The points in these coordinate systems can be denoted by $r_{p,i}$ and $r_{site,i}$, respectively, where i is the number of corresponding targets which ranges from 1 to n. The transformation can be written as follows:

$$r_{site} = sR(r_p) + T \quad (1)$$

where $R(r_p)$ is the transformed version of the initially reconstructed point cloud. Minimization of the sum of the squared errors is formulated as:

$$\sum_1^n \|e_i\|^2 = \sum_1^n \left\| r_{site,i} - sR(r_{p,i}) - T \right\|^2 \quad (2)$$

To solve for this transformation, similar to Golparvar-Fard et al. (2009), the approach proposed in Horn (1987) is used which gives a closed-form solution to the least square problem of absolute orientation. To extract the rebar intersections and calculate the safe drilling depth within each rebar cell, an algorithm (Saidi et al. 2011) was developed to automatically perform this step and reduce the data processing time.

The inputs for the algorithm are a point cloud, the radius of the rebar, an initial deck thickness, and an initial drilling direction. The algorithm segments the point cloud and identifies the rebar grid and quadrilateral cells using pattern recognition techniques. The output of this algorithm is the cell drilling depth, status of cells (safe or unsafe), and the rebar intersections.

The results from the rebar intersection extraction algorithm are further processed in order to visualize the safe drilling zones in the BIM of the rebar and embedment. The four corners of each cell generated by the above algorithm are used to generate volumes in an IFC model and that model is used to update the BIM model. The shape of the volume for safe drilling zones reflects the as-built rebar cage alignment. Volumes are only generated where it is permissible to drill through the entire depth of the rebar cage. Zones where it might be permissible to drill partially through the depth of the rebar cage are flagged as unsafe drilling zones and no volume is generated.

Figure 2: (a) data collection; (b) registration targets

Using the D^{4}AR – 4 dimensional augmented reality – modeling visualization (Golparvar-Fard et al. 2009), the resulting color-coded cells (in the form of IFC-based BIM) along with the reconstructed point cloud and registered imagery are visualized in an augmented reality environment. The outcome of this pipeline can be displayed using a laser projector on the surface of the concrete or can be used to guide drilling equipment equipped with tracking modules to identify safe/unsafe drilling areas. Figure 3 shows the data and process in our developed method.

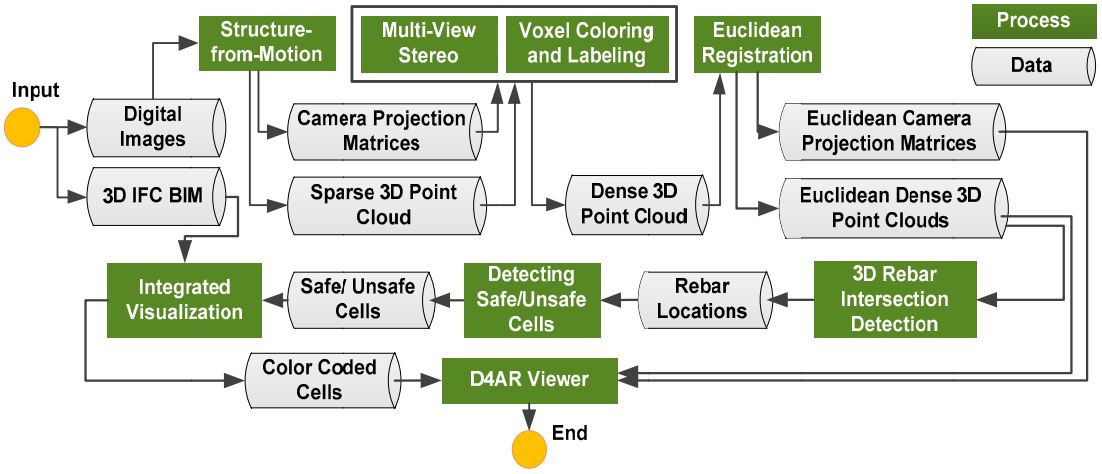

Figure 3: The data and process in our images-based 3D reconstruction, registration, rebar intersection extraction, and D^{4}AR Augmented Reality visualization

EXPERIMENTS AND DISCUSSION ON RESULTS

Data Collection and Setup

The data required for these experiments were collected in the NIST IACJS testbed wherein a mockup of the type of rebar cage found on a railway bridge deck was constructed. The reconfigurable rebar cage (R2C) was designed and fabricated to easily simulate various rebar configurations. The rebar is held rigidly within the R2C

using clamps in order to establish a reliable ground truth. The as-built configuration of the R2C uses epoxy-coated #6 rebar (i.e., 1.9 *cm* diameter). Two layers of rebar are separated by approximately 30.5 *cm* (12 *in*) and each layer consists of thirteen 3.66 *m* (12 *ft*) long rebar laid on top of twenty two 2.44 *m* (8 *ft*) long rebar. The rebar are spaced at 15.2 *cm* (6 *in*) apart within each layer and the bottom layer of rebar is also separated from the rebar cage's floor (the plywood) by 15.2 *cm* (6 *in*). We used a commercially available digital single lens reflex (SLR) camera and collected a total of 850 images. Camera and imagery specification can be found in Table 1.

Table 1. Camera Specification and Image Collection Details

Setting	Description
Camera Type	Nikon SLR Digital camera
Lens Type	20 mm – f/2.8
ISO speed	ISO 600
Images / Linear foot	1 to 2 images/linear foot
Top view images taken	50 to 70 images
Spatial resolution	Approx. 21.1 megapixels
Total # of images	850

Wide-range and close-up images were taken to minimize the visual occlusion of the bottom layer of the rebar while maintaining a normal distribution of the images across the rebar cage. To ensure all areas of the rebar cage are fully captured, the field expert slowly walked around the rebar cage and captured an average of one image per linear foot. About 50 to 70 images were also captured from the top to ensure the areas in the middle of the rebar cage were also fully documented. This strategy helped maximize the level of detail and fully document the bottom rebar layer. Figure 4 illustrates several images that were captured during the experiment.

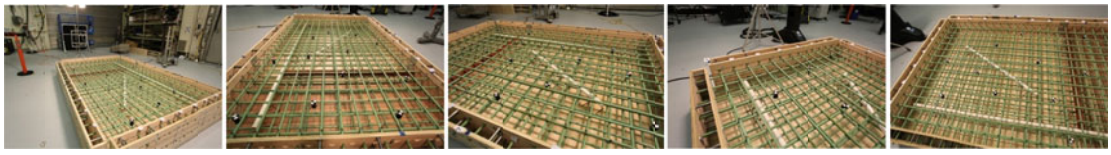

Figure 4: Several images of the rebar cage collected in the IACJS Testbed

A total of fifteen control points were used to transform the point cloud into the site coordinate system. Figure 5 illustrates the camera with an iGPS (indoor GPS) receiver unit mounted on it and three of the rebar targets. The locations of the centers of the targets were surveyed using the iGPS system. This data was used to transform each point cloud to the site coordinate system.

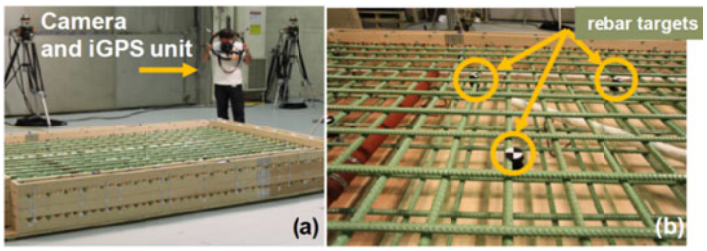

Figure 5: (a) The camera and iGPS unit in use; (b) control points

The Outcome of 3D Reconstruction and Registration

To initially test the algorithm in our experiments, we selected a subset of 380 images in which the subjects were mainly the reinforcement bars and their configurations. The spatial resolution of these images was synthetically reduced to two mega pixels to test the robustness of the proposed method to low-resolution images and to minimize the computation time. The outcome of the image-based 3D reconstruction module is shown in Figure 6. The reconstructed point cloud consists of 9,264,880 points for the entire scene. The majority of the reconstructed points as observed belong to the rebar cage. In order to transform the reconstructed point cloud to the site coordinate system, we used 15 targets with known locations. In this approach, the registration accuracy is insensitive to how the control points are selected. In the IACJS Testbed, more than three rebar targets (the minimum) were used to minimize the interactive selection errors. The resulting registration error was 0.4 *mm*. (Please refer to (Golparvar-Fard et al. 2011) for registration error computations.)

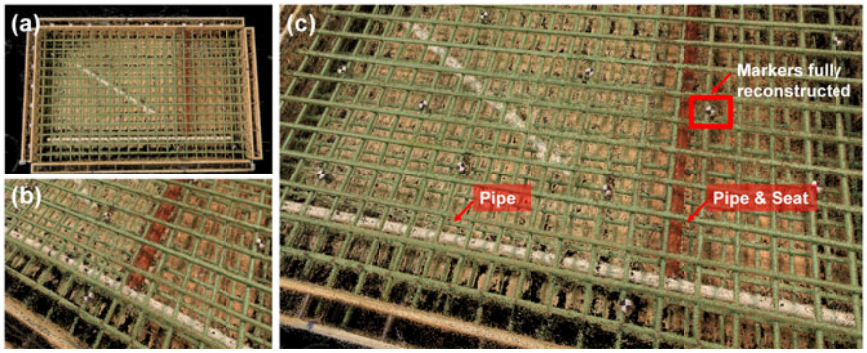

Figure 6: (a) Snap shot of the 3D reconstructed model of the test bed, (b) close snap shot of the reconstructed model, (c) pipes, seat, and markers fully reconstructed in the reconstructed 3D point cloud model.

Figure 7 shows the reconstructed point cloud superimposed with the IFC-based bridge deck BIM seen through a semi-transparent image (7a). Figure 7b shows the location of a camera in relation to the augmented scene which is post processed using the presented image-based 3D reconstruction algorithm.

Automated Identification of Safe/Unsafe Drilling Areas

Figure 8a shows the ground truth (see Saidi et al. 2011 for details) for determining the location of safe/unsafe cells. In this case, the unsafe drilling cells are shown with darker color. Figure 8b shows the outcome of the safe/unsafe drilling cell detection wherein the unsafe cells are color coded in red. As seen, several cells are not detected (seen as empty) and several False Positives resulted, some of which were due to the presence of the targets which were not initially included in the ground truth model.

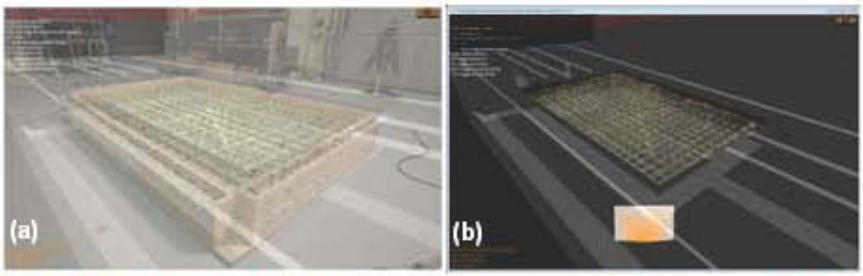

Figure 7: D[4]AR model of the expected and actual mapping of the site

Impact of Number of Images and Control Points on the Method Accuracy

In order to systematically study the impact of the number of images per unit of area on the accuracy of the reconstruction as well as the rebar and safe/unsafe cell detection, we initially divided the rebar cage plan into 4 equilaterals (Ω_k). For each, we looked into the visibility of every reconstructed point (i) and calculated the number of cameras that observe the point (C_i). Next, for each equilateral (Ω_k), the total number of cameras that observe all reconstructed points in Ω_k $(\sum_1^m C_i)_k$ is computed. The outcome is clustered into a 4-bin histogram, each bin clustering images into categories of similar contribution. In order to systematically and uniformly reduce the number of images per unit of area, in each step a percentage of images from each category was selected. As a result, several subsets of 18, 23, 127, 195, and 246 images are automatically selected. Each dataset was processed to generate a 3D point cloud. Each point cloud was transformed to the global coordinate system of the IACJS testbed and it was segmented to retain the rebar cage and remove the surrounding scene. The refined point clouds were fed into an algorithm to extract the rebar intersection and an algorithm to identify the safe/unsafe cells.

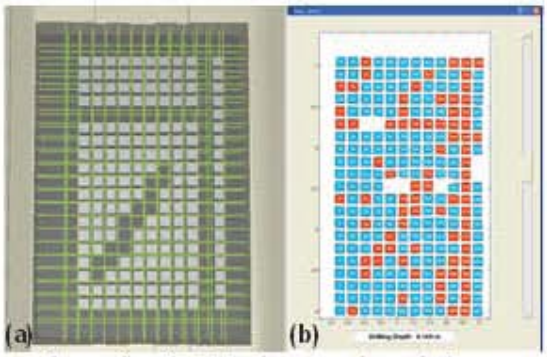

Figure 8: (a) Ground truth; (b) Undetected and detected safe/unsafe cells

Figure 9a and Figure 9b show the results of the point cloud density for the total number of images used and per unit of area (considering the visibility measurement mentioned above). In our initial experiment, we synthetically reduced the spatial resolution of images by a factor of 2 before the MVS and VCL steps. In these experiments we used the original 2 MPixel images which resulted in a significantly higher density (e.g., for 246 images per 9.3 square meter (100 square foot) of unit area, the point cloud had a density of about 50 million points). As seen in Figure 9, the density of the point cloud increases rapidly up to 127 images; however, after 127 images, increasing the number of images may not necessarily add to the density of the point cloud. This may indicate that for up to about 130 images per 9.3 square meter (100 square foot), the majority of the detail (data) is collected from the

rebar cage and additional photos yield redundant data. Hence the additional images are only contributing to the increase in the visibility metric.

We also studied the number of control points needed to accurately register the point cloud into the site coordinate system. Control points need to be non-uniformly distributed along the test bed to tighten the degree of freedom and improve the registration accuracy. This can be a function of both the number of control points and the density of the point cloud since the sparser point clouds do not accurately visualize the target and may result in registration inaccuracy. Figure 10 presents the outcome of this analysis in logarithmic scale. Our experiment on a 246 image data set demonstrates that as the number of the control points increases, the accuracy of the registration increases as well (i.e., the registration error decreases). However, after a certain number of control points (eight control points), the registration error seems to stay constant.

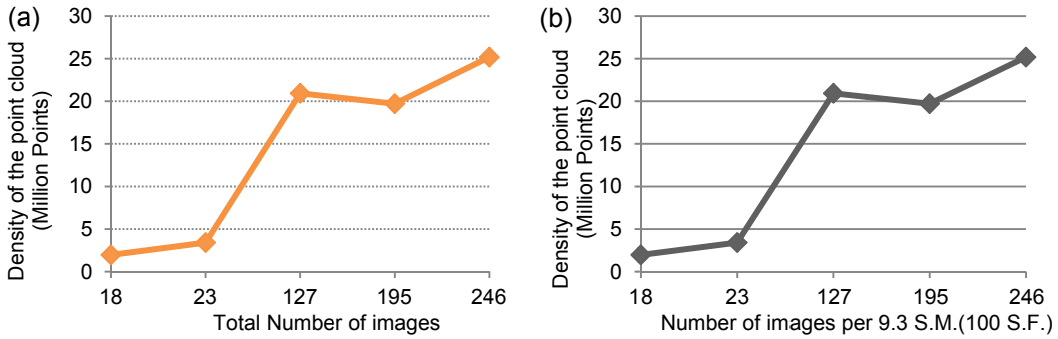

Figure 9: Density of the reconstructed point clouds vs. the number of images

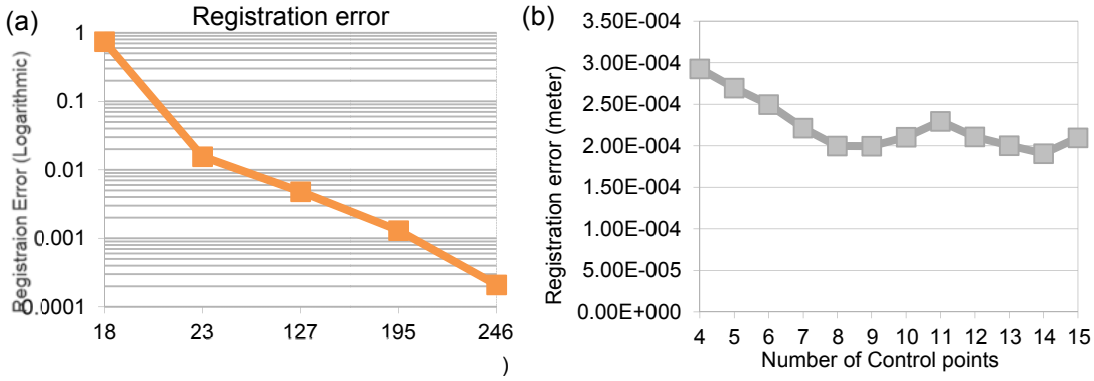

Figure 10: The accuracy of registration vs. the number of control points and images

In a subsequent set of studies, our transformed 3D point clouds were placed into the rebar intersection extraction and safe/unsafe cell identification algorithms. In those experiments where only 18 and 23 images per 9.3 square meter (100 square foot) were used, the detection algorithm failed. This is due to the pre-design threshold for the level of density in our detection algorithm. In other cases, although the density was increased, the outcome of the detection was not changed. In our experiment, this can be interpreted as the minimum number of images required per 9.3 square meter (100 square foot) which is about 130 images. More extensive experiments need to be

conducted to find the practical number of images required per unit of area to guide field engineers when collecting the imagery necessary for a proper detailed 3D mapping of rebar and embedded objects prior to placement of concrete.

CONCLUSIONS AND FUTURE WORK

In this paper we present a new image-based approach for 3D mapping the locations of the rebar and embedded objects prior to placement of concrete on a railway bridge deck. The result of our experiments shows that by only using digital images, practitioners can identify where the rebar and other embedded objects are within the bridge decks, locate safe and unsafe drilling areas, and can use the resulting 3D map to document the embedded objects for future retrofit or rehabilitation of the concrete bridge decks. We studied the impact of the number of images and control points on the accuracy and density of the image-based 3D reconstruction, registration, and automated recognition of the rebar locations and safe/unsafe cells in detail. Our result shows that this approach has the potential to bypass the need for expensive and labor-intensive laser scanning approaches.

As part of a larger study, we have looked into benchmarking the accuracy of the proposed image-based approach against the state-of-the-art laser scanners. These comprehensive experiments and their results are documented in (Saidi et al. 2011). We also need to study the impact of the camera distance and baseline between every pair of images and the applicability of video cameras on the accuracy of the proposed method. Also, developing an accurate plan for comprehensive and complete data collection needs to be explored in future work. Moreover, in future we will use precision-recall curves for evaluating the performance of our algorithm. We also need to create a new machine learning algorithm to automatically learn the threshold on the point cloud density for automated rebar and safe/unsafe cell detection. This can facilitate future data collections that may suffer from low point cloud density.

AKNOWLEDGEMENT

The authors like to thank the support and help of C. Brown, J. Swerdlow, I. Katz of NIST and M. Akula with data collection and experimental setup.

REFERENCES

Cheok, G. S., (2006). "Proc. of the 3rd NIST Workshop on Performance Evaluation of 3D Imaging Systems," *NISTIR 7357, NIST*, Gaithersburg, MD.

Furukawa Y. and Ponce J. (2010). "Accurate, dense, and robust multi-view stereopsis." *IEEE Trans. Pattern Analysis and Machine Intel.32,1362–1376.*

Golparvar-Fard M., Peña-Mora F., and Savarese S. (2011a). "Automated model-based progress monitoring using unordered daily construction photographs and IFC as-planned models." *ASCE J. of Computing in Civil Eng*. (in press).

Golparvar-Fard, M., Bohn, J., Teizer, J., Savarese, S., Peña-Mora, F., (2011b), "Evaluation of image-based modeling and laser scanning accuracy for emerging automated performance monitoring techniques." *J. of AutoCon,* 20(8), 1143-115.

Golparvar-Fard, M., Peña-Mora, F., & Savarese, S. (2009). D4AR - A 4-Dimensional Augmented Reality Model for Automating Construction Progress Data Collection, Processing and Communication. *J. of ITCON, 14*, 129-153.

Horn, B. (1987). Closed-form Solution of Absolute Orientation using Unit Quatemions. *J. of the Optical Society, A(4)*, 629-642.

Lowe D. (2004). "Distinctive image features from scale-invariant keypoints." *Int. J. of Computer Vision*, 60 (2), 91-110.

Saidi, K., Cheok, G., Franaszek, M., Brown, C., Swerdlow, J., Lipman, R., Katz, I., Golparvar-Fard, M., Goodrum, P., Akula, M., Dadi, G., and Ghadimi, B. (2012), "Development and Use of the NIST Intelligent and Automated Construction Job Site Testbed". *NIST TN 1726*, National Institute of Standards and Technology, Gaithersburg, MD, Dec, 2011.

Snavely N., Seitz S.M., and Szeliski R. (2006). "Photo Tourism: Exploring Photo Collections in 3D," *ACM Trans. Graphics*, 835-846.

Tang, P., Huber, D., Akinci, B., Lipman, R., Lytle, A. (2010). "Automatic reconstruction of as-built building information models from laser-scanned point clouds: a review of related techniques." *J. of AutoCon*, 19, 829-843.

Whitfield, C. R. (2010). 3D Scanning: Embrace Mobile 3D Laser Scanning. *Prof Survys*.